PNAS RESEARCH ARTICLE | CHEMISTRY

The gas|liquid interface eclipses the liquid|liquid interface for glucose oxidase rate acceleration in microdroplets

Lynn E. Krushinski[a,1], Patrick J. Herchenbach[a,1], and Jeffrey E. Dick[a,b,2]

Edited by Veronica Vaida, University of Colorado Boulder, Boulder, CO; received August 12, 2024; accepted October 8, 2024

The curious chemistry observed in microdroplets has captivated chemists in recent years and has led to an investigation into their ability to drive seemingly impossible chemistries. One particularly interesting capability of these microdroplets is their ability to accelerate reactions by several orders of magnitude. While there have been many investigations into which reactions can be accelerated by confinement within microdroplets, no study has directly compared reaction acceleration at the liquid|liquid and gas|liquid interfaces. Here, we confine glucose oxidase, one of life's most important enzymes, to microdroplets and monitor the turnover rate of glucose by the electroactive cofactor, hexacyanoferrate (III). We use stochastic electrochemistry to monitor the collision of single femtoliter water droplets on an ultramicroelectrode. We also develop a measurement modality to robustly quantify reaction rates for femtoliter liquid aerosol droplets, where the majority of the interface is gas|liquid. We demonstrate that the gas|liquid interface accelerates enzyme turnover by over an order of magnitude over the liquid|liquid interface. This is the first apples-to-apples comparison of reaction acceleration at two distinct interfaces that indicates that the gas|liquid interface plays a central role in driving curious chemistry.

electrochemistry | microdroplet | enzyme

Significance

Recent literature has demonstrated that microdroplets can accelerate chemical reactions by orders of magnitude. There is currently debate surrounding which interfaces, such as the liquid|liquid versus the gas|liquid, are most potent at accelerating reactions. Unfortunately, no measurement technique to date has been able to successfully probe these two interfaces to provide a distinct quantitative comparison. Here, we use stochastic electrochemistry to show that the discrete microdroplet|gas interface is superior to the liquid|liquid interface at accelerating glucose oxidase enzymatic rates. This work extends the conversation of reaction acceleration to important biochemical reactions occurring at complex phase boundaries.

Microdroplets have recently captivated the scientific community as confined reaction vessels that can perform unlikely chemistries not observed in bulk. From their ability to spontaneously promote typically unfavorable reactions (1–8) to their effect on key biological and environmental processes (9–16), microdroplets have been implicated in a multitude of interesting reactions, even those central to the origins of life (17). Of particular interest is the ability of microdroplets to accelerate reactions by several orders of magnitude (18–23). Typically, reaction acceleration in microdroplets is studied in electrospray or atomized microdroplets in gas and the gas|liquid interface is implicated as essential to the observed acceleration (24–26). Our group has previously shown that this curious chemistry extends to enzyme kinetics affected by the liquid|liquid interface, where an enzymatic reaction (FADGDH oxidation of glucose) confined in emulsion droplets can accelerate turnover rates of the enzyme by two orders of magnitude. We further showed that the rate increases inversely with droplet radius (27). While there have been reports of reaction acceleration promoted both by the gas|liquid and liquid|liquid interfaces, there has yet to be a direct comparison of a single reaction for the two interfaces. This is because methods typically suitable for analysis of droplets in gas (i.e., mass spectrometry) do not extend to emulsion droplets or droplets in oil. Recently, our group detailed a method for the analysis of single aerosolized droplets with a novel electrochemical cell, extending electrochemistry to the gas|liquid interface (28).

In this report, we detail the first direct comparison of reaction acceleration of the same reaction for the liquid|liquid and gas|liquid interfaces. Here, we confine a more familiar enzyme, glucose oxidase, to microdroplets containing the substrate (glucose) and the electrochemically active cofactor (hexacyanoferrate (II)) to create a system that can be observed via electrochemistry. This enzymatic system was monitored both in droplets in oil (with the previously reported method (27)) and droplets in gas with an adaptation of the electrochemical cell mentioned above for the capture and analysis of aerosol droplets (28). Both methods allow for the determination of enzyme turnover rate on a droplet-by-droplet basis (as opposed to an ensemble measurement of average acceleration). This report marks the first direct comparison between reaction acceleration of the same chemical system in droplets in oil (liquid|liquid interface) and droplets in gas (gas|liquid interface). Through this investigation, we reveal that the gas|liquid interface leads to higher reaction acceleration by nearly an order of magnitude for all measured droplet sizes.

Results and Discussions

To create an electrochemical cell capable of analyzing aerosol particles in their native state (i.e., without dilution), a platinum wire working electrode (d = 100 μm) was placed in an ionic liquid droplet (~50 μL) that was pipetted onto a platinum foil, which acted as the

Author affiliations: [a]Department of Chemistry, Purdue University, West Lafayette, IN 47907; and [b]Elmore Family School of Electrical and Computer Engineering, Purdue University, West Lafayette, IN 47907

Author contributions: L.E.K., P.J.H., and J.E.D. designed research; L.E.K. and P.J.H. performed research; L.E.K., P.J.H., and J.E.D. analyzed data; and L.E.K., P.J.H., and J.E.D. wrote the paper.

The authors declare no competing interest.

This article is a PNAS Direct Submission.

[1]L.E.K. and P.J.H. contributed equally to this work.

[2]To whom correspondence may be addressed. Email: jdick@purdue.edu.

This article contains supporting information online at https://www.pnas.org/lookup/suppl/doi:10.1073/pnas.2416353121/-/DCSupplemental.

Published December 9, 2024.

quasireference & counter electrode (QRCE, h = 0.25 mm). A schematic of this electrochemical cell can be seen in Fig. 1*A*. This system was adapted from our previous work, where a cylindrical electrode threaded through a suspended ionic liquid collector acted as the working electrode for single liquid aerosol interrogation. We also showed that the aerosol sizes realized from the electrochemical data aligned well with results from a commercial particle sizer (28). In this work, an ionic liquid, 1-butyl-3-methylimidazolium hexafluorophosphate (BMIM-PF_6), droplet acted as a hydrophobic collector volume where intact aerosol droplets and their contents could interact with the working electrode without being significantly absorbed or diluted. The working electrode used was a platinum wire (d = 100 μm) partially sealed within a glass capillary for stability. An example of a working electrode used for these experiments along with electrochemical characterization is in *SI Appendix*, Fig. S1.

For the enzymatic experiments, the above electrochemical system was used to analyze aerosol droplets that contained the enzyme of interest, glucose oxidase, the substrate, glucose, and the precursor for the electrochemically generated cofactor, hexacyanoferrate (II). Our droplets are loaded with 200 mM buffer at pH 6.6 to ensure no significant pH changes during the oxidation of glucose. Thus, we do not expect pH fluctuations imposed by aerosolization. In our studies, we chose hexacyanoferrate due to its high solubility in water and lack of partitioning into 1,2-dichloroethane. We expect other more bioavailable redox molecules to lead to similar trends. When such an aerosol droplet contacts the working electrode [biased sufficiently (0.5 V. vs. Pt foil QRCE) to oxidize hexacyanoferrate (II)], the enzymatic cofactor hexacyanoferrate (III) is generated. This process results in a sudden current spike. After generation of the cofactor, glucose oxidase is then able to turn over glucose within the droplet (to glucanolactone) and regenerate hexacyanoferrate (II), which can then be reoxidized at the electrode surface. This catalytic process creates an observable limiting current when the transients are observed via amperometry (Fig. 1*B*). Because the native cofactor of glucose oxidase is oxygen, all experiments were performed in a deoxygenated chamber to ensure the enzymatic reaction is dependent on the electrogenerated hexacyanoferrate (III). In addition, argon was used as the carrier gas for the nebulization of glucose oxidase-containing aerosols. The particle size distribution for aerosols generated under such conditions can be seen in *SI Appendix*, Fig. S2, where the average particle diameter was determined to be ~1 μm, but a distribution of droplets exists from 5 to 45 μm. The applied potential for these experiments was determined from cyclic voltammetry taken before and after ~1 min of nebulization of hexacyanoferrate (II) containing aerosols onto the electrochemical cell where the observed half-wave potential was ~0.3 V vs. Pt foil QRCE (*SI Appendix*, Fig. S3). Thus, 0.5 V vs. Pt foil QRCE was chosen because it was a sufficient overpotential to ensure the oxidation of hexacyanoferrate (II) at mass-transfer limitation without any other background processes (i.e., water oxidation). After a sufficient potential was chosen, amperometry was performed during the active nebulization of aerosols that contained hexacyanoferrate (II) and glucose in phosphate buffer with or without added enzyme. Example amperograms taken during the nebulization of aerosols with and without added enzyme can be seen in *SI Appendix*, Fig. S5. Without added enzyme, the transients show an exponential decay, characteristic of hexacyanoferrate (II) oxidation in aerosols as shown in our previous report (28). The integration of these transients can be related to the aerosol size as explained in (*SI Appendix*, Fig. S4) and the average calculated aerosol size was determined to be 12 ± 6 μm (N = 50), with the aerosol sizes ranging from 3 to 30 μm (*SI Appendix*, Fig. S2). These results align with the larger distribution of droplets measured with the particle sizer, as mentioned above (*SI Appendix*, Fig. S2). These results indicate that the analysis of individual aerosol droplets in this system is possible.

For the enzyme-containing experiments, the droplet volume and the turnover rate (k_{turn}) of the enzyme within the droplet can be determined from the characteristic transients (Fig. 1*B*). The derivation of equations used for these values stems from a previous publication on the determination of enzymatic rates in droplets (27). Briefly, the observed limiting current (which is corrected by the background current) can be related to the turnover rate of the droplet by

$$k_{turn} = \frac{i_{lim}}{qnC_{enzyme}V_{aerosol}N_A}, \quad [1]$$

where k_{turn} is the turnover rate of the enzyme within the aerosol, i_{lim} is the background-subtracted limiting current of the transient, q is the elementary charge of an electron, n is the number of electrons involved in the enzymatic reaction (2), C_{enzyme} is the concentration of the enzyme in the aerosol droplet, $V_{aerosol}$ is the volume of the aerosol (relevant equation below), and N_A is Avogadro's number. The volume of the aerosol ($V_{aerosol}$) can be determined using

$$V_{aerosol} = \frac{Q}{F\left(n_1 C_{glucose} + n_2 C_{hexacyanoferrate(II)}\right)}, \quad [2]$$

where Q is the integrated charge of the transient, F is Faraday's constant, n_1 is the number of electrons involved in glucose oxidation(2), $C_{glucose}$ is the concentration of glucose, n_2 is the number

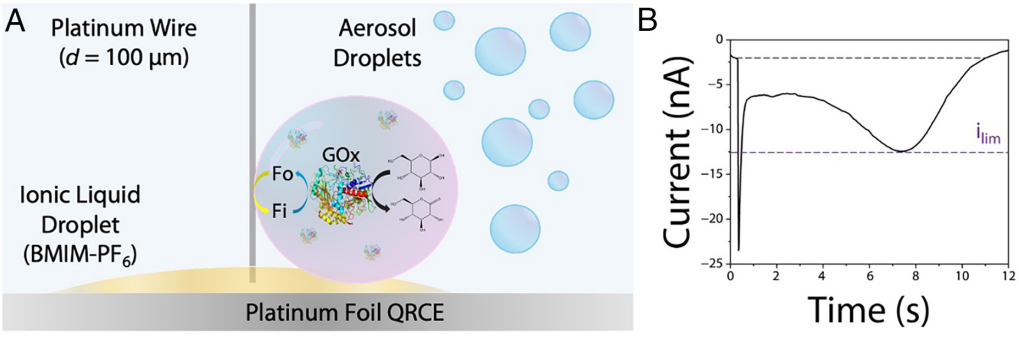

Fig. 1. (*A*) Schematic of experimental set-up. Aerosol droplets containing glucose, glucose oxidase, and hexacyanoferrate (II) [Fo] are sprayed at a platinum wire working electrode in contact with an ionic liquid droplet on a platinum foil (h = 0.25 mm) quasireference & counter electrode. (*B*) Current vs time plot for a single aerosol droplet colliding with the platinum working electrode. The limiting current (purple dashed line) was corrected by the background current (black dashed line).

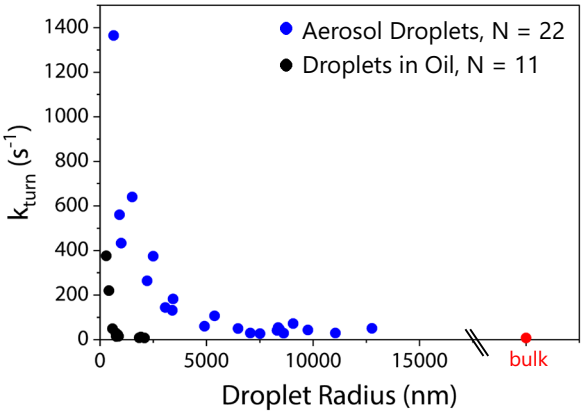

Fig. 2. Plot of calculated k_{turn} values versus droplet radius in oil (black dots, N = 11) and aerosol droplets (blue dots, N = 22). The bulk (2 mL solution volume) k_{turn} value was determined to be 0.44 + 0.07 s^{-1}.

of electrons involved in hexacyanoferrate (II) oxidation (1), and $C_{hexacyanoferrate(II)}$ is the concentration of hexacyanoferrate (II).

It should be noted that only the very first transient observed during amperometry was used for droplet volume and k_{turn} determination. This is because after an initial transient is observed, the aerosol responsible will act as a collector volume for future impacting aerosols. While a droplet volume and k_{turn} determination could be made from future transients, the values would not report on true values as there would be some dilution by the parent aerosol responsible for the first transient rendering the values inaccurate. Because of this, each amperometric experiment with enzyme-containing aerosols was only performed until the first transient was observed (and not for a set time interval). Example transients obtained and analyzed in this fashion and the calculated values can be seen in *SI Appendix*, Fig. S6. The values were then plotted as k_{turn} vs. aerosol radius, and the resulting plot can be seen in Fig. 2. Values for the measurements of the k_{turn} determined for glucose oxidase in bulk solution (2 mL) and aqueous droplets in oil can also be seen in Fig. 2. The bulk k_{turn} was determined via amperometry (*SI Appendix*, Fig. S7) and UV-vis spectroscopy (*SI Appendix*, Fig. S8) as outlined in our previous work (27). From these experiments, the bulk k_{turn} value was determined to be 0.44 ± 0.07 s^{-1}. For the droplets in oil, the same droplet solution used for the aerosol experiments was ultrasonicated in an oil phase (100 mM tetrabutylammonium perchlorate in DCE) to give rise to microdroplets suspended in oil, as previously reported (27). Examples of analyzed transients and the resulting k_{turn} and droplet radius values for the droplets in oil can be found in *SI Appendix*, Fig. S9.

While the observed dependence of k_{turn} on aerosol radius mimics the trend observed for droplets in oil (27), the observed acceleration factor in these experiments (maximum calculated k_{turn} divided by the bulk k_{turn}) is ~3,000. This means that the observed turnover rate for glucose oxidase confined to small aerosol droplets (~1 μm diameter) is over three orders of magnitude greater than the observed value in bulk. It should be noted that the minimum aerosol size that can be observed by this method is limited by the noise in the background of the measurement (from the nebulization of aerosols), and droplets smaller than 1 μm in diameter are difficult to observe. For droplets in oil, droplet sizes of 100 s of nm are easily observable (27). Even with a smaller range of droplet sizes accessible, the maximum observed acceleration factor in these experiments was ~100. In general, the observed k_{turn} in aerosol droplets are an order of magnitude larger than those for droplets in oil, even for droplets which are considerably large (>20 μm radius). The k_{turn} values for similarly sized droplets in gas and oil as well as the bulk k_{turn} value are plotted in Fig. 3*A*. Here, a ~900 nm radius droplet has a calculated k_{turn} value of 560 and 15 s^{-1} for aerosol droplets and droplets in oil, respectively. While the observation that aerosol droplets, which have a gas|liquid interface, promote glucose oxidase turnover rate acceleration an order of magnitude greater than droplets in oil, which have a liquid|liquid interface, may seem striking, several groups have previously discussed the possibility of this phenomenon (21, 22, 29–31). However, directly correlated measurements that probe both a liquid|liquid and gas|liquid interface have not been previously accessible. With the observations reported herein, we are able to demonstrate that the gas|liquid interface promotes greater reaction acceleration than the liquid|liquid interface.

The notion that the gas|liquid interface promotes stronger reaction acceleration than the liquid|liquid interface can have several possible explanations (32). First, the electric field strength at the gas|liquid interface (~10^9 V/cm) is proposed to be two orders of magnitude greater than the liquid|liquid interface (~10^7 V/cm) (6, 25, 26, 33, 34). This proposed field strength may play a large role in observed reaction acceleration (21, 22, 30, 33, 35). Second, molecular organization and pH gradients at the interface are thought to be more pronounced at the gas|liquid than the liquid|liquid interface (29, 30, 36). This interfacial pH at complex interfaces likely plays a key role in the overall acceleration mechanism (37, 38). For instance, this pH may facilitate enzymatic adsorption to the phase boundary. Previously, Ben-Amotz has

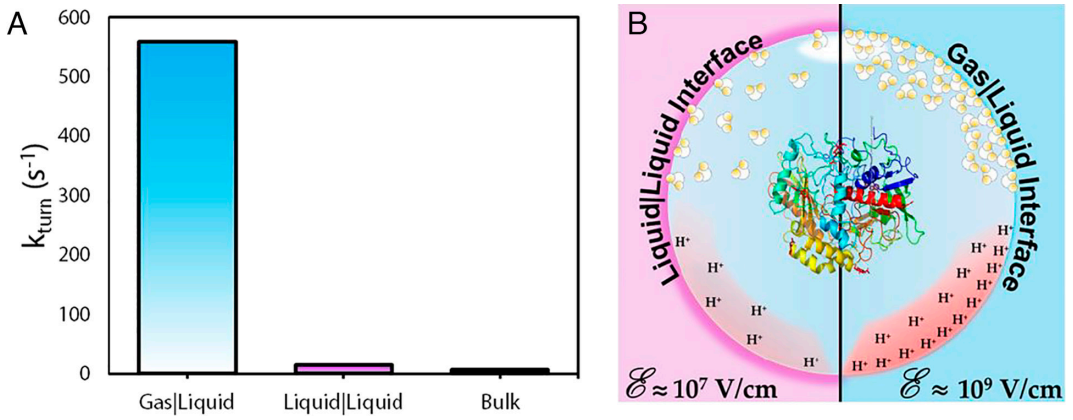

Fig. 3. (*A*) k_{turn} values for droplets of similar size for droplets in gas (blue bar, r = 915 nm) and droplets in oil (purple bar, r = 875 nm) (*B*) Schematic demonstrating the differences between the gas|liquid and liquid|liquid interfaces.

demonstrated the importance of reactant versus product adsorption affinity to the phase boundary in reaction acceleration (39). Many of these physicochemical considerations, including the role of the interfacial electric field, are likely at play and responsible for enzymatic rate enhancement. Such factors, shown in Fig. 3*B*, could potentially affect the organization of glucose oxidase, and its active site, at the interface, making substrate binding more favorable.

Conclusion

Recently, many groups have reported on reaction acceleration and other curious chemistry that occurs in confined microdroplets (40–49). Enzymes have traditionally been studied in bulk solutions, however their native environment is confined within cells. Here, we use a novel electrochemical cell to probe enzymatic reaction kinetics in microdroplets in oil and microdroplets in gas. While the gas|liquid interface has been thought to increase reaction rates more than the liquid|liquid interface, this is the first direct comparison between droplets with the same chemical system at different interfaces. We found that the reaction rate of glucose oxidase was increased in droplets in gas by over an order of magnitude, implying the importance of this interface compared to the liquid|liquid interface. In aggregate, our results indicate the importance that multiphase boundaries, especially under confinement, have in key biochemical processes, which may have direct implications to reaction acceleration and cellular compartmentalization (50–52). This finding adds direct evidence to the hypothesis that the gas|liquid interface accelerates reactions much more than the liquid|liquid interface.

Materials and Methods

Reagents and Materials. Potassium ferricyanide (99+%, ACS reagent), Platinum wire, 0.1 mm (0.004in) dia, Premion™, 99.997% (metals basis), Platinum foil, 0.25 mm (0.01in) thick, 99.95% (metals basis), and potassium phosphate dibasic (98+%, ACS reagent) were purchased form Thermo Scientific. All reagents were used as is without further purification. Sulfuric acid (Certified ACS grade), hydrogen peroxide (ACS grade), potassium chloride (99%), and potassium phosphate monobasic (Certified ACS) were purchased from Fisher Chemical. Gallium (99.9% trace metal basis), potassium hexacyanoferrate (II) trihydrate (≥99.95% trace metals basis), dextrose (meets EP, BP, JP, USP testing specifications, anhydrous), 1-Butyl-3-methylimidazolium hexafluorophosphate (BMIM-PF_6, for catalysis, ≥98.5%), tetrabutylammonium perchlorate ([TBA][ClO4], for electrochemical analysis, >99.0%), 1,2-dichloroethane (DCE, 98%), and glucose oxidase from *Aspergillus niger* (Type VII, lyophilized powder, ≥100,000 units/g solid (without added oxygen)) were purchased from Sigma Aldrich. 22AWG silicone hook up wire (OD: 1.7 mm)–22 gauge stranded tinned copper wire with silicone insulation, six colors (black, red, yellow, green, blue, white) 23 ft/7 m each, hook up wire kit from Plusivo was used for making electrical connection to the fabricated electrodes. Borosilicate glass capillaries (O.D.: 1.0 mm, I.D.: 0.50 mm) were purchased from Sutter Instruments. All aqueous solutions were prepared in ultrapure water (Millipoer Milli-Q, 18.2 MΩ cm). 200 mM phosphate buffer was prepared with 200 mM potassium phosphate monobasic, 200 mM potassium phosphate dibasic, and 200 mM potassium chloride and was sonicated using an Ultrasonic Cleaner with Digital Timer (VWR, Radnor, Pennsylvania) until all solid was dissolved. The buffer pH was determined to be 6.6 with an Orion VeraStar Pro Advanced electrochemistry Monitor (Thermo Scientific). All enzyme concentrations were corrected by the reported purity of the enzyme (60%) and all prepared enzyme solutions were kept refrigerated after preparation and remade fresh after ~5 h. All electrochemical experiments were performed on a CH Instruments 6284E potentiostat. Experiments were performed in a deoxygenated chamber which was kept under constant Argon purging. The chamber used for these experiments was a modified Precise Basic Glove Box (Labconco) with fittings created for the potentiostat leads and other wiring. Cylindrical platinum electrodes were positioned with a Line Tool Co. A LH linear micropositioner. Henry Schein Nebulizers Adult Mouthpiece Ea, 50 EA/CA (PN-1118D) purchased from Grayline Medical were used for the nebulization of aerosols for all experiments. A Grimm Aerosol Spectrometer 11-D ("The Dust Decoder") was used for aerosol sizing. A Vernier Go Direct SpectroVis Plus was used for the determination of bulk k_{turn} via UV-vis spectroscopy.

Fabrication and Characterization of Cylindrical Platinum Electrodes. Platinum wire electrodes were fabricated by sealing a ~3 cm platinum wire (d = 100 μm) into a borosilicate glass capillary (O.D.: 1.0 mm, I.D.: 0.50 mm, Sutter Instruments). The glass capillary was partially sealed by exposing the threaded capillary to a propane torch (Benzomatic) for several seconds. A portion of the threaded wire should be left exposed at the end of the capillary (typically ~2 to 3 mm of wire was left exposed). The resulting electrode should have a portion of wire exposed, a portion sealed within the capillary, and a portion left unsealed within the capillary (such that electrical connection can be made). After the platinum wire was sealed as described, electrical wire (Plusivo [purchased through Amazon]) which was dipped in gallium (stored at 55 °C to maintain a liquid state) was then threaded into the capillary to make electrical connection. The electrical wire was secured in place with heat-sealed plastic (Plusivo [purchased through Amazon]). All electrodes were cleaned in concentrated piranha solution (3:1 sulfuric acid: hydrogen peroxide) before use. The electrodes were then tested via cyclic voltammetry in a solution containing 2.5 mM hexacyanoferrate (II/III) in 250 mM KCl by scanning from −0.1 to 0.5 V vs. Ag/AgCl at a scan rate of 100 mV/s. An example of a fabricated electrode as well as the electrochemical characterization can be seen in *SI Appendix*, Fig. S1.

Determination of Bulk k_{turn} with Amperometry and UV-vis Spectroscopy. A stock solution of 2.5 mM hexacyanoferrate (III) and 100 mM glucose in 200 mM phosphate buffer was prepared for both methods. Then, 2 mL of the stock solution was either added to a vial or a cuvette for amperometry and UV-vis spectroscopy, respectively. A stock solution of 0.1 mM glucose oxidase was prepared in 200 mM phosphate buffer and was kept refrigerated between measurements. In all measurements, 50 μL of stock enzyme solution was spiked in after approximately 60 s. For amperometry, a CHI Au UME (r = 6.25 μm) was used as a working electrode, a Pt wire [0.25 mm diameter] (Alfa Aesar, Stoughton, MA) was used as the counter electrode and an Ag/AgCl (CH Instruments, Austin, Texas) reference electrode connected by a salt bridge (1 M KCl suspended in agarose) was used. Amperometry was held at 0.5 V vs. Ag/AgCl for 1,800 s with the solution being stirred on a battery-powered stir-plate. For UV-vis spectroscopy, an excitation wavelength of 420 nm was used and a plastic cuvette with a 1 cm pathlength was used. All experiments were performed in a deoxygenated chamber under constant argon purging.

Aerosol Electroanalysis. Solutions of 2.5 mM hexacyanoferrate(II) 100 mM glucose both with and without ~0.2 mM glucose oxidase were prepared in 200 mM phosphate buffer. All solutions were nebulized with argon within the deoxygenated chamber (described above) with a Henry Schein Nebulizer. A new nebulizer was used for each solution. The Pt foil quasireference counter electrode and platinum wire working electrode were cleaned with Millipore water between experiments. To prepare the electrochemical cell used for these experiments, a 50 μL droplet of ionic liquid was pipetted onto the platinum foil (connected to the reference and counter leads of the potentiostat) and a platinum wire working electrode was placed into the ionic liquid droplet with a Line Tool Co. micropositioner such that a portion of the wire was submerged into the droplet (but not touching the Pt foil QRCE) and another portion was left exposed (such that it could interact with incoming aerosols). For each amperometric i–t experiment, amperometry was run for 400 total seconds, where background amperometry in the ionic liquid droplet was taken for ≈20 s before solution nebulization. The solution was then nebulized for the remaining amperometry time, with the nebulizer held ≈5 in. from the electrochemical cell. For enzyme containing experiments, amperometry was ended when a transient was observed. Sizing of the liquid aerosols was performed with a Grimm 11-D Aerosol Spectrometer and electroanalytical techniques.

Collision Experiments with Droplets in Oil. A solution of 2.5 mM hexacyanoferrate(II) 100 mM glucose both and 0.25 mM glucose oxidase was prepared in 200 mM phosphate buffer. Then, 15 μL of the enzyme solution was pipetted into 2 mL of a continuous oil phase (100 mM TBAP in DCE) and the solution was

ultrasonicated (500 W, 40% amplitude) for 5 s with a horn sonicator (QSONICA Q500, 6.4-mm diameter tip). A gold ultramicroelectrode (CHI, $r = 6.25$ μm) was used as the working electrode, a platinum wire ($d = 0.5$ mm) was used as a counter electrode, and an Ag/AgCl reference electrode (CHI) was connected via a salt bridge. Chronoamperometry was run on a CHI 6284E potentiostat with a 0.45 V starting potential and a 0.5 V final potential for a single step which was 300 s at a sample rate of 0.0167 s. The working electrode was polished by a brief soak in 1 M HNO_3 followed by 1 min of polishing on a clean polishing pad wet with Milli-Q water (BASi).

Data, Materials, and Software Availability. All study data are included in the article and/or supporting information.

ACKNOWLEDGMENTS. This work was completed with financial support from the Chemical Measurement and Imaging Program in the NSF Division of Chemistry under Grant CHE-2403964. We would like to acknowledge Azaria Wagner for assistance with nebulization experiments. J.E.D. would like to acknowledge Elizavyeta Sofia Dick, whose inspirational curiosity in 2021 sent us down the pathway of making measurements in bubbles.

1. M. A. Mehrgardi, M. Mofidfar, R. N. Zare, Sprayed water microdroplets are able to generate hydrogen peroxide spontaneously. *J. Am. Chem. Soc.* **144**, 17 (2022). 10.1021/jacs.2c02890.
2. L. E. Krushinski, J. E. Dick, Direct electrochemical evidence suggests that aqueous microdroplets spontaneously produce hydrogen peroxide. *Proc. Natl. Acad. Sci. U.S.A.* **121**, e2321064121 (2024). 10.1073/pnas.2321064121.
3. L. Qiu, R. G. Cooks, Spontaneous oxidation in aqueous microdroplets: Water radical cation as primary oxidizing agent. *Angew. Chem. Int. Ed.* **63**, e202400118 (2024). 10.1002/anie.202400118.
4. L. Qiu, R. G. Cooks, Simultaneous and spontaneous oxidation and reduction in microdroplets by the water radical cation/anion pair. *Angew. Chem. Int. Ed.* **61**, 41 (2022). 10.1002/anie.202210765.
5. J. K. Lee, D. Samanta, H. G. Nam, R. N. Zare, Micrometer-sized water droplets induce spontaneous reduction. *J. Am. Chem. Soc.* **141**, 27 (2019). 10.1021/jacs.9b03227.
6. S. Jin *et al.*, The spontaneous electron–mediated redox processes on sprayed water microdroplets. *JACS Au.* **3**, 6 (2023). 10.1021/jacsau.3c00191.
7. M. F. Ruiz-Lopez, J. S. Francisco, M. T. C. Martins-Costa, J. M. Anglada, Molecular reactions at aqueous interfaces. *Nat. Rev. Chem.* **4**, 459–475 (2020). 10.1038/s41570-020-0203-2.
8. E. C. Griffith, V. Vaida, In situ observation of peptide bond formation at the water-air interface. *Proc. Natl. Acad. Sci. U.S.A.* **109**, 39 (2012). 10.1073/pnas.1210029109.
9. I. Nam, H. G. Nam, R. N. Zare, Abiotic synthesis of purine and pyrimidine ribonucleosides in aqueous microdroplets. *Proc. Natl. Acad. Sci. U.S.A.* **115**, 36–40 (2017). 10.1073/pnas.1718559115.
10. J. K. Nam, H. G. Lee, R. N. Nam, Zare, Abiotic production of sugar phosphates and uridine ribonucleoside in aqueous microdroplets. *Proc. Natl. Acad. Sci. U.S.A.* **114**, 12396–12400 (2017). 10.1073/pnas.1714896114.
11. B. K. Spoorthi *et al.*, Spontaneous weathering of natural minerals in charged water microdroplets forms nanomaterials. *Science* **384**, 1012–1017 (2024). 10.1126/science.adl3364.
12. D. T. Holden, N. M. Morato, R. G. Cooks, Aqueous microdroplets enable abiotic synthesis and chain extension of unique peptide isomers from free amino acids. *Proc. Natl. Acad. Sci. U.S.A.* **119**, e2212642119 (2022). 10.1073/pnas.2212642119.
13. W. Wang *et al.*, Water microdroplets allow spontaneously abiotic production of peptides. *J. Phys. Chem. Lett.* **12**, 5774–5780 (2021). 10.1021/acs.jpclett.1c01083.
14. G. B. Ellison, A. F. Tuck, V. Vaida, Atmospheric processing of organic aerosols. *J. Geophys. Res. Atmos.* **104**, 11633–11641 (1999). 10.1029/1999JD900073.
15. D. J. Donaldson, V. Vaida, The influence of organic films at the air-aqueous boundary on atmospheric processes. *Chem. Rev.* **106**, 1445–1461 (2006), 10.1021/cr040367c.
16. A. M. Deal, R. J. Rapf, V. Vaida, Water–air interfaces as environments to address the water paradox in prebiotic chemistry: A physical chemistry perspective. *J. Phys. Chem. A* **125**, 4929–4942 (2021). 10.1021/acs.jpca.1c02864.
17. The Tuck, role of atmospheric aerosols in the origin of life. *Surv. Geophys.* **23**, 11864–11868 (2002). 10.1023/A:1020123922767.
18. S. Banerjee, E. Gnanamani, X. Yan, R. N. Zare, Can all bulk-phase reactions be accelerated in microdroplets? *Analyst* **142**, 1399–1402 (2017). 10.1039/c6an02225a.
19. M. F. Ruiz-López, M. T. C. Martins-Costa, Disentangling reaction rate acceleration in microdroplets. *Phys. Chem. Chem. Phys.* **24**, 29700–29704 (2022). 10.1039/d2cp04998h.
20. K. J. Vannoy, M. Q. Edwards, C. Renault, J. E. Dick, An electrochemical perspective on reaction acceleration in droplets. *Annu. Rev. Anal. Chem.* **17**, 149–171 (2024). 10.1146/annurev-anchem-061622-030919.
21. Z. Wei, Y. Li, R. G. Cooks, X. Yan, Accelerated reaction kinetics in microdroplets: Overview and recent developments. *Annu. Rev. Phys. Chem.* **71**, 31–51 (2020). 10.1146/annurev-physchem-121319-110654.
22. X. Yan, R. M. Bain, R. G. Cooks, Organic reactions in microdroplets: Reaction acceleration revealed by mass spectrometry. *Angew. Chem. Int. Ed.* **55**, 12960–12972 (2016). 10.1002/anie.201602270.
23. J. K. Lee, S. Banerjee, H. G. Nam, R. N. Zare, Acceleration of reaction in charged microdroplets. *Q. Rev. Biophys.* **48**, 439–448 (2015). 10.1017/S0033583515000086.
24. Z. Song *et al.*, Deciphering the microdroplet acceleration factors of aza-Michael addition reactions. *J. Am. Chem. Soc.* **146**, 10963–10972 (2024). 10.1021/jacs.4c02312.
25. H. Hao, I. Leven, T. Head-Gordon, Can electric fields drive chemistry for an aqueous microdroplet? *Nat. Commun.* **13**, 1–10 (2022). 10.1038/s41467-021-27941-x.
26. H. Xiong, J. Kyoo Lee, R. N. Zare, W. Min, Strong electric field observed at the interface of aqueous microdroplets. *J. Phys. Chem. Lett.* **11**, 7423–7428 (2020). 10.1021/acs.jpclett.0c02061.
27. K. J. Vannoy, I. Lee, K. Sode, J. E. Dick, Electrochemical quantification of accelerated FADGDH rates in aqueous nanodroplets. *Proc. Natl. Acad. Sci. U.S.A.* **118**, e2025726118 (2021). 10.1073/pnas.2025726118.
28. L. E. Krushinski, K. J. Vannoy, J. E. Dick, Single liquid aerosol microparticle electrochemistry on a suspended ionic liquid film. *Small* **20**, 2308637 (2024). 10.1002/smll.202308637.
29. L. Qiu, Z. Wei, H. Nie, R. G. Cooks, Reaction acceleration promoted by partial solvation at the gas/solution interface. *ChemPlusChem* **86**, 1361–1368 (2021). 10.1002/cplu.202100373.
30. Q. Ge *et al.*, Significant acceleration of photocatalytic CO2 reduction at the gas–liquid interface of microdroplets. *Angew. Chem. Int. Ed.* **62**, e202304189 (2023). 10.1002/anie.202304189.
31. Y. B. Vogel *et al.*, The corona of a surface bubble promotes electrochemical reactions. *Nat. Commun.* **11**, 6323 (2020). 10.1038/s41467-020-20186-0.
32. G. Rovelli *et al.*, A critical analysis of electrospray techniques for the determination of accelerated rates and mechanisms of chemical reactions in droplets. *Chem. Sci.* **11**, 13026–13034 (2020). 10.1039/d0sc04611f.
33. P. J. Heindel, H. Hao, R. Allen LaCour, T. Head-Gordon, Spontaneous formation of hydrogen peroxide in water microdroplets. *J. Phys. Chem. Lett.* **13**, 10035–10041 (2022). 10.1021/acs.jpclett.2c01721.
34. C. F. Chamberlayne, R. N. Zare, Simple model for the electric field and spatial distribution of ions in a microdroplet. *J. Chem. Phys.* **152**, 184702 (2020). 10.1063/5.0006550.
35. J. K. Lee *et al.*, Spontaneous generation of hydrogen peroxide from aqueous microdroplets. *Proc. Natl. Acad. Sci. U.S.A.* **116**, 19294–19298 (2019). 10.1073/pnas.1911883116.
36. M. Ahmed *et al.*, Molecular properties and chemical transformations near interfaces. *J. Phys. Chem. B* **125**, 9037–9051 (2021), 10.1021/acs.jpcb.1c03756.
37. R. J. Rapf, M. R. Dooley, K. Kappes, R. J. Perkins, V. Vaida, PH dependence of the aqueous photochemistry of α-keto acids. *J. Phys. Chem. A* **121**, 8798–8805 (2017). 10.1021/acs.jpca.7b08192.
38. M. Ruiz-Bermejo, C. Menor-Salván, S. Osuna-Esteban, S. Veintemillas-Verdaguer, Prebiotic microreactors: A synthesis of purines and dihydroxy compounds in aqueous aerosol. *Orig. Life Evol. Biosph.* **37**, 123–131 (2007). 10.1007/s11084-006-9026-5.
39. D. Ben-Amotz, Interfacial chemical reactivity enhancement. *J. Chem. Phys.* **160**, 084701 (2024). 10.1063/5.0186945.
40. J. Ghosh, J. Mendoza, R. G. Cooks, Accelerated and concerted aza-Michael addition and SuFEx reaction in microdroplets in unitary and high-throughput formats. *Angew. Chem. Int. Ed.* **61**, e202214090 (2022). 10.1002/anie.202214090.
41. H. Cheng, S. Tang, T. Yang, S. Xu, X. Yan, Accelerating electrochemical reactions in a voltage-controlled interfacial microreactor. *Angew. Chem. Int. Ed.* **59**, 19862–19867 (2020). 10.1002/anie.202007736.
42. K. H. Huang, N. M. Morato, Y. Feng, R. G. Cooks, High-throughput diversification of complex bioactive molecules by accelerated synthesis in microdroplets. *Angew. Chem. Int. Ed.* **62**, e202300956 (2023). 10.1002/anie.202300956.
43. B. Chen *et al.*, Water-solid contact electrification causes hydrogen peroxide production from hydroxyl radical recombination in sprayed microdroplets. *Proc. Natl. Acad. Sci. U.S.A.* **119**, e2209056119 (2022). 10.1073/pnas.2209056119.
44. K. H. Huang, Z. Wei, R. G. Cooks, Accelerated reactions of amines with carbon dioxide driven by superacid at the microdroplet interface. *Chem. Sci.* **12**, 2242–2250 (2021). 10.1039/d0sc05625a.
45. J. K. Lee *et al.*, Condensing water vapor to droplets generates hydrogen peroxide. *Proc. Natl. Acad. Sci. U.S.A.* **117**, 30934–30941 (2020). 10.1073/pnas.2020158117.
46. A. F. Tuck, Gibbs free energy and reaction rate acceleration in and on microdroplets. *Entropy* **21**, 1044 (2019). 10.3390/e21111044.
47. C. M. Dobson, G. B. Ellison, A. F. Tuck, V. Vaida, Atmospheric aerosols as prebiotic chemical reactors. *Proc. Natl. Acad. Sci. U.S.A.* **97**, 11864–11868 (2000). 10.1073/pnas.200366897.
48. E. C. Griffith, A. F. Tuck, V. Vaida, Ocean–atmosphere interactions in the emergence of complexity in simple chemical systems. *Acc. Chem. Res.* **45**, 2106–2113 (2012). 10.1021/ar300027q.
49. J. Lee, F. P. Cakmak, R. Booth, C. D. Keating, Hybrid protocells based on coacervate-templated fatty acid vesicles combine improved membrane stability with functional interior protocytoplasm. bioRxiv [Preprint] (2024) 10.1101/2024.08.06.606659 (Accessed 16 October 2024).
50. A. Fallah-Araghi *et al.*, Enhanced chemical synthesis at soft interfaces: A universal reaction-adsorption mechanism in microcompartments. *Phys. Rev. Lett.* **112**, 028301 (2014). 10.1103/PhysRevLett.112.028301.
51. C. D. Keating, Aqueous phase separation as a possible route to compartmentalization of biological molecules. *Acc. Chem. Res.* **45**, 2114–2124 (2012). 10.1021/ar200294y.
52. K. R. Wilson *et al.*, A kinetic description of how interfaces accelerate reactions in micro-compartments. *Chem. Sci.* **11**, 8533–8545 (2020). 10.1039/d0sc03189e.